

terested in the electrostatic potential generated by the aluminosilicate framework and partly because not all Na sites are fully occupied in the "average" structure, but full occupancy must be the case for any specific Na interaction with the framework.

The most important result to be learned from these maps is the *shape* of the aluminosilicate framework. It is characterized by a large positive potential around each of the nuclei and looks very much like a model of the structure constructed with overlapping spheres. It is nothing like the pictures of  $\phi(r)$  constructed by assuming point charges at the atomic sites (e.g., see calculations by Preuss, Linden, and Peuckert<sup>17</sup>). We believe our mapping of  $\phi(r)$  in Figure 2 is more realistic, except for reservations we have concerning neglect of the Na atoms. For a more detailed study it would be necessary to include the contribution of the Na<sup>+</sup> ions.

Regions of chemical interest in  $\phi(r)$  are the areas of minimum potential and high electric field (i.e., steep slope of  $\phi(r)$ ). In Figure 2c there are shallow minima inside the 6-ring associated with the O(3) atoms. In the 8-ring (Figure 3d) there are minima associated with all O atoms, but it is easy to see that a Na ion (or atom) would more readily occupy the site (2) (close to one O(2) and two O(1) atoms) rather than close to one O(1) and two O(2) atoms. The Na(2) fractional site population of 0.23 (0.01) suggests that almost every 8-ring has a Na atom bound inside it.

Perhaps the most interesting section for  $\phi(r)$  mapping is that through the large cavity (Figure 2a). The Na(3) atom lies in the center of a broad, flat area of low potential in the mapped plane. The minima in this plane are at top left ( $-0.48 \text{ e } \text{\AA}^{-1}$ ) and right of center on the top of the map ( $-0.64 \text{ e } \text{\AA}^{-1}$ ). The right-hand corner of the map ( $1/4, 1/4, 1/4$ ) is a local maximum ( $-0.19 \text{ e } \text{\AA}^{-1}$ ). Thus, a point charge would experience a barrier of  $0.45 \text{ e } \text{\AA}^{-1}$ , or  $625 \text{ kJ mol}^{-1}$ , to movement across the cavity. This is not expected to be a realistic estimate of diffusion energies through the structure. Even if  $\phi(r)$  were being mapped reliably, the diffusing particles are not point charges, and their interaction energy with the aluminosilicate framework would be an integral over a substantial region of space. Moreover, a diffusing particle

need not pass directly through the center of the large cavity. Instead, it could move closer to the walls (i.e., the oxygen atoms) where the electrostatic potential is virtually constant.

Although we do not give maps of the electric field in the cavities, we can derive  $E(r)$  (a vector quantity) from  $\phi(r)$  readily, and it can be expressed in a similar way to  $\phi(r)$  (eq 1) as a combination of Fourier and direct space summations (e.g., see ref 11). As shown elsewhere for stishovite,<sup>11</sup> direct mapping of  $E(r)$  via this strategy is not likely to be accurate. Rather, we would prefer to derive a pseudoatom model representation of  $\rho(r)$ , and from this extract  $E(r)$ , essentially with no thermal motion. However, as we discuss below, this approach requires a more extensive data set than that analyzed here.

### Conclusions and Future Prospects

This work is intended as a feasibility study, to show how much information on bonding electron densities and electrostatic properties in the zeolite structures can be extracted from low-resolution X-ray data. The results are promising. However, we defer a comparison with results on other mineral systems, or with theoretical calculations, until more extensive X-ray data are available. The data should extend to  $\sin \theta/\lambda \geq 1.0 \text{ \AA}^{-1}$ , requiring shorter wavelength (Mo or Ag), which in turn would further reduce effects of extinction on the low-angle data. Also, it would be desirable to collect the X-ray data at reduced temperatures. Since the zeolite crystals are generally soft and have large open structures, thermal motion is much higher than in simple minerals. For example,  $B_{\text{eq}}$  values for Si ( $1.85 (3) \text{ \AA}^2$ ), Al ( $1.97 (3) \text{ \AA}^2$ ), and O ( $3.0 \text{ \AA}^2$ ) are far higher than observed in quartz [ $0.49 \text{ \AA}^2$  (Si) and  $0.99 \text{ \AA}^2$  (O)<sup>18</sup>] and corundum [ $0.23 \text{ \AA}^2$  (Al) and  $0.27 \text{ \AA}^2$  (O)<sup>3</sup>] at room temperature.

*Acknowledgment.* We thank Prof. B. Craven for encouragement and criticisms, and we are grateful to Mrs. Joan Klinger for technical assistance. Dr. J. Pluth, University of Chicago, kindly supplied the zeolite A data. This work was supported in part by a grant (HL-20350) from the National Institutes of Health.

(17) Preuss, E.; Linden, G.; Peuckert, M. *J. Phys. Chem.* **1985**, *89*, 2955-2961.

(18) LePage, Y.; Calvert, L. D.; Gabe, E. J. *J. Phys. Chem. Solids* **1980**, *41*, 721.

## Adsorption and Decomposition of HCOOH on Potassium-Promoted Rh(111) Surfaces

Frigyes Solymosi,\* János Kiss, and Imre Kovács

*Reaction Kinetics Research Group of the Hungarian Academy of Sciences and Institute of Solid State and Radiochemistry, University of Szeged, P.O. Box 105, H-6701 Szeged, Hungary (Received: May 20, 1987)*

Preadsorbed potassium significantly altered the adsorption and the reactions of HCOOH on Rh(111) surface. A potassium-induced desorption peak of HCOOH was identified, with  $T_p = 254 \text{ K}$ . Preadsorbed potassium enhanced the dissociation of HCOOH and stabilized a formate species characterized by the photoemission peaks at 5.2, 8.9, 10.3, and 12.2 eV in the He II spectrum. These peaks were eliminated at 267 K on clean Rh, at 330 K at  $\theta_K \approx 0.1$ , and above 422 K with a monolayer of potassium ( $\theta_K = 0.36$ ). Decomposition of the formate species led to the formation of H<sub>2</sub>, CO<sub>2</sub>, H<sub>2</sub>O, and CO, which desorbed at significantly higher temperatures than from the K-free surface. In the interpretation of the effects of potassium, an extended charge transfer between HCOOH and the K/Rh(111) surface (at  $\theta_K \approx 0.1$ ) and a direct chemical interaction between potassium and HCOOH involving the formation of potassium formate like species ( $\theta_K \approx 0.36$ ) are assumed.

### Introduction

In a previous paper we investigated the interaction of HCOOH with clean and oxygen-dosed Rh(111) surfaces.<sup>1</sup> As pointed out earlier,<sup>1,2</sup> there is a strong evidence that the formate species is an important surface intermediate in the formation of oxygenated carbon compounds over Rh. In the present study we report on

the influence of potassium on the adsorption and decomposition of HCOOH on Rh(111); this is strongly connected with a program relating to evaluation of the effects of potassium additive in the hydrogenations of CO and CO<sub>2</sub> on Rh catalyst. As part of this program, the effects of potassium have been examined on the

\* Address correspondence to this author at Reaction Kinetics Research Group, The University of Szeged, H-6701 Szeged, P.O. Box 105, Hungary.

(1) Solymosi, F.; Kiss, J.; Kovács, I. *Surf. Sci.* **1987**, *192*, 47.  
(2) Deluzarche, A.; Hindermann, J. P.; Kieffer, R.; Kiennemann, A. *Rev. Chem. Intermed.* **1985**, *6*, 625.

adsorption of  $\text{CO}_2$ ,<sup>3</sup>  $\text{H}_2$ ,<sup>4</sup>  $\text{H}_2\text{O}$ ,<sup>4</sup> and  $\text{CH}_3\text{OH}$ <sup>5</sup> over Rh(111). Apart from a short report,<sup>6</sup> the influence of an alkali metal additive on the interaction of HCOOH with clean metal surfaces has not been investigated previously.

### Experimental Section

The UHV system used in these experiments is equipped for temperature-programmed desorption (TPD), Auger electron spectroscopy (AES), and low-energy electron diffraction (LEED). TD spectra were taken in "line of sight" with a heating rate of  $10 \text{ K s}^{-1}$ . In order to obtain stoichiometric information from TDS the relative mass spectrometer sensitivities and differences in pumping speed were taken into account. UPS measurements were performed in another system, where photoelectrons were detected with an electrostatic hemispherical energy analyzer (Leybold Hereaus LHS 10). This system also contained AES facility. The same Rh sample was used in both chambers. Experimental details, including the cleaning of the Rh(111) sample, were described in our previous paper.<sup>1</sup> The sample was cleaned between each individual experiment. Potassium was deposited on the Rh(111) surface by heating a commercial SAES Getter source situated 3 cm from the sample. After several days' degassing of a K source at a flowing current of 4–6 A, a clean evaporated K layer was obtained on the Rh surface. The determination of K coverage is described in our other work.<sup>3</sup> Changes in work function were obtained from He I UPS spectrum.

### Results

**1. Thermal Desorption Measurements.** In the first series of measurements, we investigated the effects of the potassium coverage on the desorption of HCOOH, and on the formation of the decomposition products. The exposure of HCOOH was 6 langmuirs which was sufficient to produce a saturation layer ( $\beta$ ) on a clean surface. TD spectra are shown in Figures 1 and 2, while the concentrations of adsorbed and desorbed species as function of the coverage are plotted in Figure 3. Figure 1A shows that, as the value of  $\theta_K$  increased, the temperature of the HCOOH peak ( $\beta$ ) shifted to higher values. The amount of weakly adsorbed HCOOH ( $\alpha$ ) gradually decreased with increase of the potassium concentration (always at the same HCOOH exposure: 6 langmuirs). At about  $\theta_K = 0.38$ , the development of the  $\alpha$  peak ceased. The appearance of this state at monolayer K coverage ( $\theta_K = 0.36$ ) required a 3 times larger HCOOH exposure than on the clean surface (Figure 1B). The amount of HCOOH desorbed in the  $\beta$  state first increased up to  $\theta_K = 0.15$ , and then gradually decreased. The  $\beta$  peak became very broad, undoubtedly consisting of at least two peaks,  $\beta_1$  and  $\beta_2$ .

As regards the desorption of  $\text{CO}_2$ , a well-reproducible decrease in the peak temperature of  $\text{CO}_2$  desorption ( $\beta$ ) was exhibited between  $\theta_K = 0.0$  and  $0.1$ , from 286 to 255 K, followed by a slight increase. This peak became very small at slightly more than monolayer K coverage, at  $\theta_K = 0.4$ . From  $\theta_K = 0.26$ , new high-temperature peaks developed, at 580 ( $\gamma_1$ ), 660 ( $\gamma_2$ ), and 706 ( $\gamma_3$ ) K (Figure 2A). They became larger at higher K coverages. The amount of  $\text{CO}_2$  formed increased with increase of the K coverage, up to about  $\theta_K = 0.08$ , then remained constant (Figure 3).

The characteristics of  $\text{H}_2$  desorption were only slightly altered up to  $\theta_K = 0.09$  (Figure 2B). Above this value, however, a well-shaped peak developed at 280 K ( $\alpha$ ) and the  $\beta$  peak became very broad. The amount of  $\text{H}_2$  varied with the potassium coverage in a similar fashion as that of  $\text{CO}_2$  (Figure 3). The ratio of  $\text{H}_2/\text{CO}_2$  was approximately 1 in the whole region of the K coverage.

A significant increase in the formation of  $\text{H}_2\text{O}$  was also experienced on K-dosed surfaces. The  $\text{H}_2\text{O}$  peak at  $T_p = 263 \text{ K}$  became larger, and above  $\theta_K = 0.07$  a new high-temperature peak

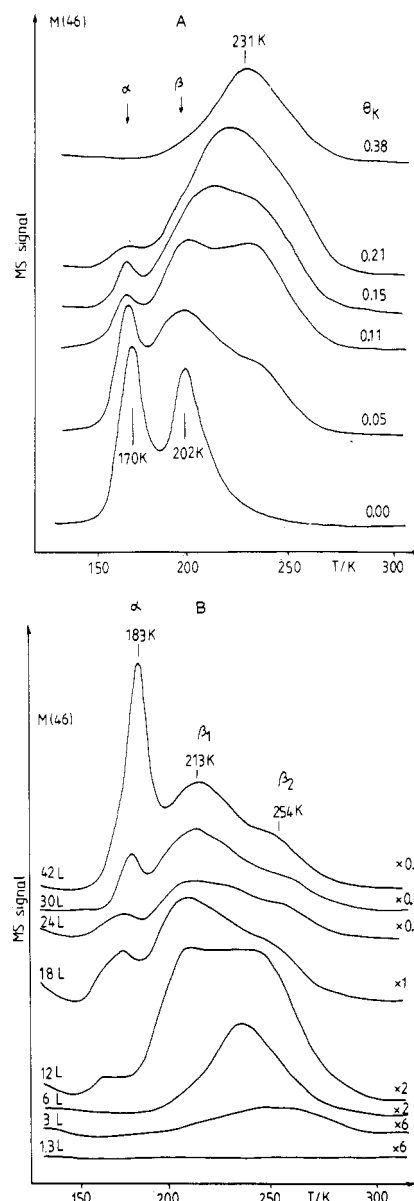


Figure 1. (A) Effects of potassium coverage and (B) HCOOH exposure on the thermal desorption of HCOOH. Adsorption temperature,  $T_a$ , was 100 K. HCOOH exposure was 6 langmuirs in (A).  $\theta_K$  was 0.33 in (B).

was produced at 371–403 K, with another one at 566 K above  $\theta_K = 0.23$  (see Figure 2C). At monolayer K coverage, the amount of  $\text{H}_2\text{O}$  produced was  $\sim 6$  times larger than that desorbed from the K-free Rh.

The striking effect of the potassium coverage is reflected in the formation of CO, too. The peak temperature for the desorption markedly increased from 522 K (K-free surface) to 670 K at  $\theta_K = 0.09$  and it reached its highest value, 706 K, even at  $\theta_K = 0.16$  (Figure 2D). Here too, the amount of CO desorbed at monolayer K coverage was about 6 times larger than in the case of the K-free surface (Figure 3).

Figure 3 presents plots of surface concentration of adsorbed HCOOH, the amounts of products formed, and their ratios as functions of the K coverage.

In the next series of measurements, the effect of HCOOH exposure was examined on the characteristics of thermal desorption at  $\theta_K = 0.33$ . In the case of HCOOH desorption, it was clearly observed that the new high-temperature adsorption state ( $\beta_2$ ) was formed first with  $T_p \approx 253 \text{ K}$ . On further increase of the HCOOH exposure, the  $\beta_1$  peak and then the  $\alpha$  peak appeared at slightly higher temperatures than for the K-free surface (Figure 1B). These characteristics were also observed at  $\theta_K = 0.1$ .

In the case of  $\text{CO}_2$  desorption, first the two high-temperature peaks ( $\gamma_2$ ,  $\gamma_3$ ) at 637 and 683 K developed. Their peak tem-

(3) Solymosi, F.; Bugyi, L. *Faraday Symp. Chem. Soc.* **1986**, *7*, 21.

(4) Berkó, A.; Kovács, I.; Solymosi, F., to be published.

(5) Berkó, A.; Tarnóczy, T. I.; Solymosi, F. *Surf. Sci.* **1987**, *189/190*, 238.

(6) Solymosi, F.; Kiss, J.; Kovács, I. *J. Vac. Sci. Technol.*, **A** **1987**, *5*, 1108.

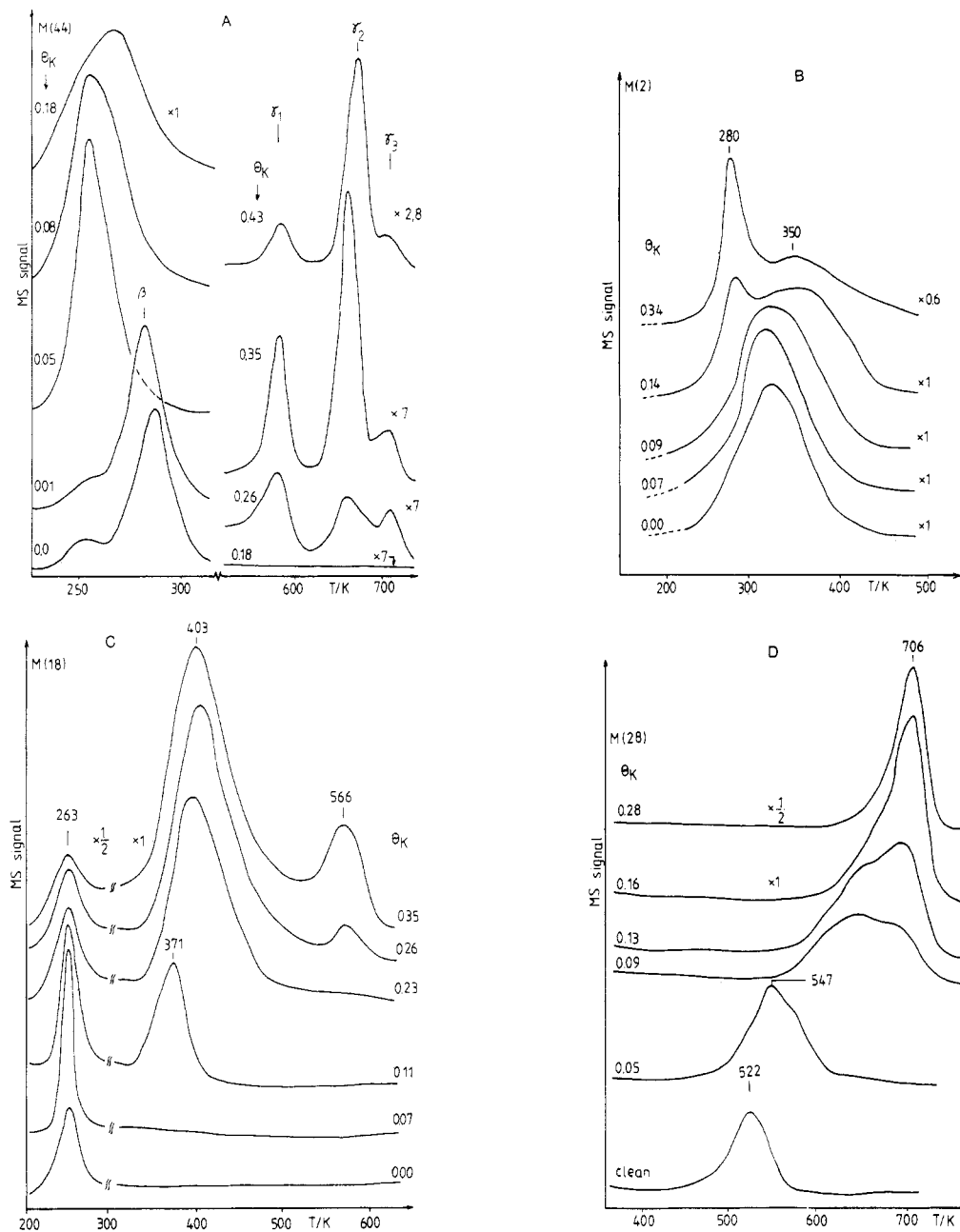


**Figure 2.** Effects of potassium coverage on the desorption of CO<sub>2</sub> (A), H<sub>2</sub> (B), H<sub>2</sub>O (C), and CO (D). HCOOH exposure was 6 langmuirs.  $T_a = 100$  K.

temperatures shifted to higher values with increase of the HCOOH exposure and the  $\gamma_2$  became the dominant peak. Above 1.5 langmuirs, the  $\gamma_1$  peak at 583 K also appeared (Figure 4A).

Similar features were exhibited by the H<sub>2</sub> desorption. An asymmetric peak with  $T_p = 483$  K appeared at low exposures. On increase of the HCOOH exposure, the peak ( $T_p = 280$  K) was formed and continuous desorption occurred between 330 and 500 K, without any distinct desorption states (Figure 4B). As follows from the results plotted in Figure 5A, the desorption of H<sub>2</sub>O occurred in a new  $\gamma$  state ( $T_p \sim 572$ –600 K). At higher HCOOH exposure another desorption state ( $\beta$ ) developed at 480 K. This peak significantly shifted to lower temperatures with the increase of the coverage indicating a second-order kinetics. A very small  $\alpha$  peak at 263 K was also detected at each exposure. Independently of the HCOOH dose, the peak temperature for CO was always 700–706 K at this K coverage (Figure 5B).

As the spectra presented in Figure 6 show, not only does potassium stabilize HCOOH and its decomposition products on Rh(111), but these adsorbed species markedly increase the binding energy of potassium to Rh(111). Above 0.6 langmuir of HCOOH exposure, the desorption observed in the lower temperature range

completely ceased and potassium mostly desorbed in two peaks, at 590 and 690 K.

Kinetic data on the thermal desorptions are collected in Table I.

**2. UPS Studies.** The deposition of potassium on Rh(111) led to an attenuation of the Rh valence-band emission. A comparison of the spectra of clean and K-covered ( $\theta_K \approx 0.36$ ) Rh samples showed that K adsorption induced a weak new broad feature centered at 5.7 eV binding energy. A similar feature has been observed in other systems: K/Fe(110),<sup>7</sup> Na/Ag(110),<sup>8</sup> K/Ni(100),<sup>9</sup> K/Ru(001),<sup>10</sup> and K/Cu(100).<sup>11</sup>

The effects of K on the adsorption of HCOOH were examined at low ( $\theta_K = 0.1$ ) and high ( $\theta_K = 0.3$ ) potassium coverages. Figures 7 and 8 show photoemission spectra of adsorbed HCOOH

(7) Broden, G.; Bonzel, H. P. *Surf. Sci.* **1979**, *84*, 106.

(8) Briggs, D.; Marbrow, R. A.; Lambert, R. M. *Surf. Sci.* **1977**, *65*, 314.

(9) Sun, Y. M.; Luftman, H. S.; White, J. M. *Surf. Sci.* **1984**, *139*, 379.

(10) Eberhardt, W.; Hoffmann, F.; DePaola, R.; Heskett, D.; Strathy, I.; Plummer, E. W.; Moser, H. R. *Phys. Rev. Lett.* **1985**, *54*, 1856.

(11) Heskett, D.; Strathy, I.; Plummer, E. W. *Phys. Rev. B* **1985**, *32*, 6222.

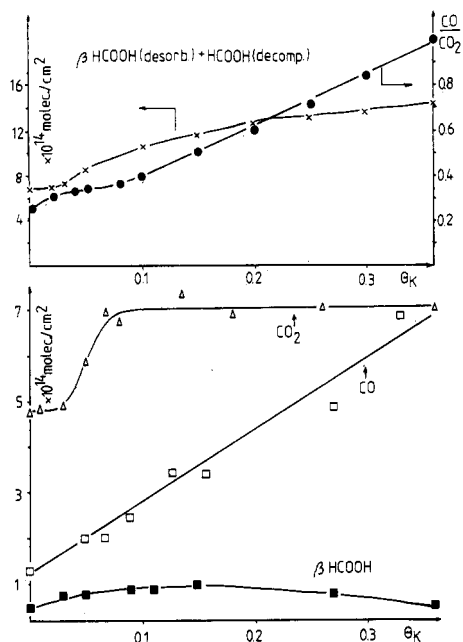


Figure 3. The surface concentration of adsorbed HCOOH ( $\beta$  and total) and the amounts of its decomposition products as a function of  $\theta_K$ . HCOOH exposure was 6 langmuirs.  $T_a = 100$  K.

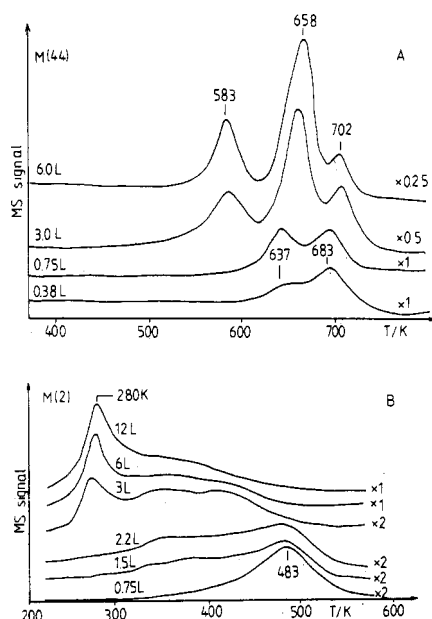


Figure 4. Effects of HCOOH exposure on the formation of CO<sub>2</sub> (A), and H<sub>2</sub> (B) at  $\theta_K = 0.33$ .  $T_a = 100$  K.

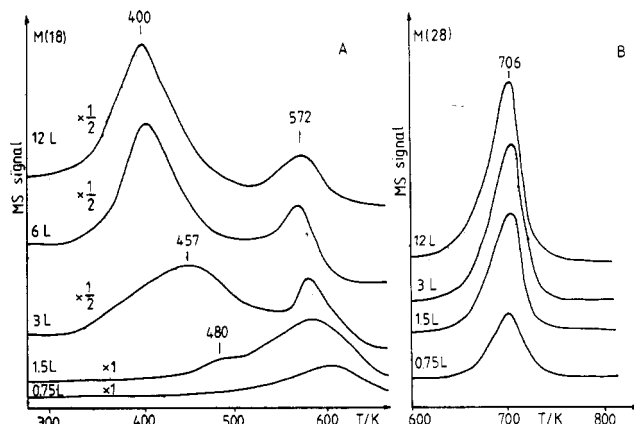


Figure 5. Effects of HCOOH exposure on the formation of H<sub>2</sub>O (A) and CO (B) at  $\theta_K = 0.33$ .  $T_a = 300$  K.

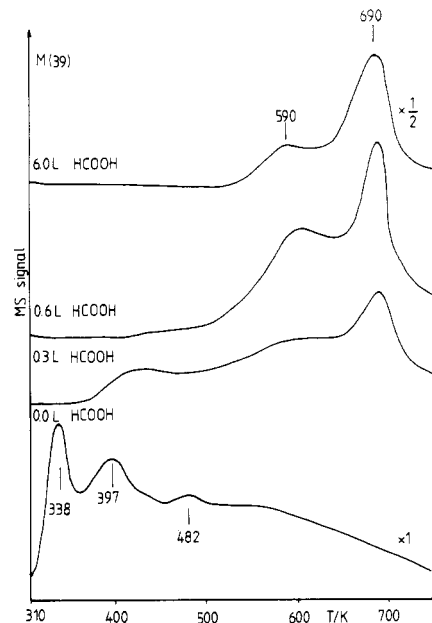


Figure 6. Desorption of potassium from clean and HCOOH-covered Rh(111) surface.  $\theta_K = 0.36$ .

TABLE I: Summary of the Results of TD Measurements after Adsorption of HCOOH at 100 K at Saturation on Potassium-Dosed Rh(111) ( $\theta_K = 0.36$ )

products	$T_p$ /K	$E^a$ /kJ mol <sup>-1</sup>
HCOOH ( $\alpha$ )	183	31.6 <sup>b</sup>
HCOOH ( $\beta_1$ )	213	51.3
HCOOH ( $\beta_2$ )	254	61.5
CO <sub>2</sub> ( $\beta$ )	260	63.0
CO <sub>2</sub> ( $\gamma_1$ )	583	145.2
CO <sub>2</sub> ( $\gamma_2$ )	658	165.1
CO <sub>2</sub> ( $\gamma_3$ )	702	175.9
CO	706	175.4
H <sub>2</sub> ( $\alpha$ )	280	65.5
H <sub>2</sub> ( $\beta$ )	483	87.4 <sup>c</sup>
H <sub>2</sub> O ( $\alpha$ )	257	65.8
H <sub>2</sub> O ( $\beta$ )	400	58.9 <sup>c</sup>
H <sub>2</sub> O ( $\gamma$ )	572	171.9 <sup>c</sup>

<sup>a</sup> Calculated from the observed values of  $T_p$  with a preexponential factor of  $10^{13}$  s<sup>-1</sup>. The accuracy of the determination of the  $T_p$  values was  $\pm 2$  K. <sup>b</sup> Calculated from the logarithm of desorption rate at the leading edge plotted against  $1/T$ . <sup>c</sup> Calculated from peak width and temperature at which the maximum rate of desorption occurs. The value was calculated at low HCOOH exposure.

and the effect of subsequent heating to higher temperatures. Spectra characteristic of the chemisorbed HCOOH appeared at 158 K. The positions of the peaks (6.2, 9.1, 10.5, and 12.0 eV) were only slightly different from those observed for the K-free surface.<sup>1</sup>

At  $\theta_K = 0.1$ , the 12.0-eV peak disappeared at around 204 K and a new peak developed at 14.2 eV. At the same time, the peak initially centred at 6.2 eV shifted to 5.2 eV. These changes correspond to the desorption of formic acid and to the formation of a formate species.<sup>1,12-15</sup> A significant increase in the intensity of the emission of the K(3p) peak at 17.4 eV also occurred, which can be seen in the difference spectra (Figure 7B). No further spectral changes appeared up to 244 K. Above this temperature, all four peaks (5.2, 8.9, 10.3, and 14.2 eV) started to attenuate. The elimination of the four-peak structure, indicating the completion of surface decomposition, occurred at 300–362 K, where two new peaks developed ( $\sim 362$  K) at 8.4 and 11.9 eV. These

(12) Joyner, R. W.; Roberts, M. W. *Proc. R. Soc. London A* **1976**, *350*, 107.

(13) Barteau, M. A.; Madix, R. J. *Surf. Sci.* **1982**, *120*, 262.

(14) Sexton, B. A.; Hughes, A. E.; Avery, N. R. *Surf. Sci.* **1985**, *155*, 366.

(15) Bowker, M.; Madix, R. J. *Surf. Sci.* **1981**, *102*, 542.

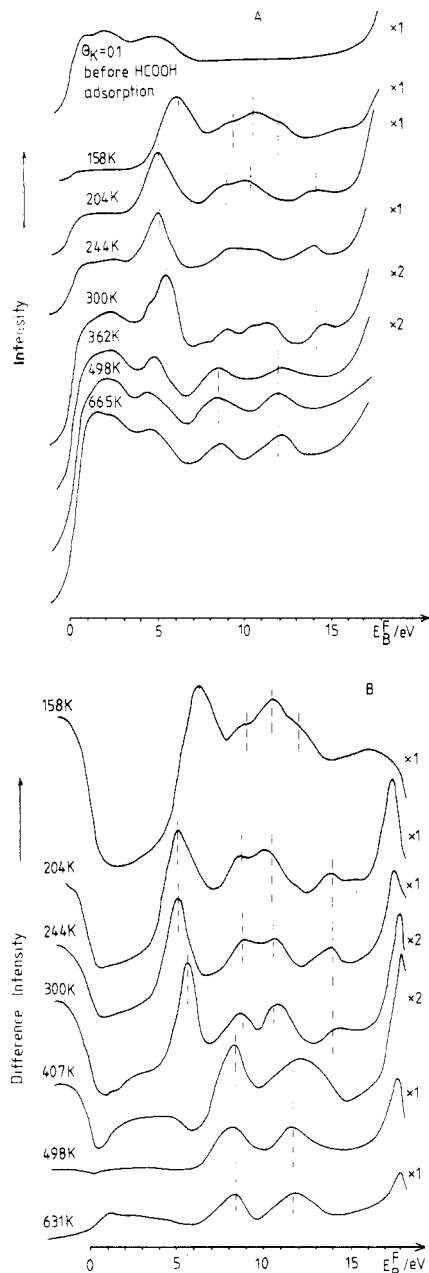


**Figure 7.** Effects of heating on the He II photoemission spectra of adsorbed HCOOH (A). Difference spectra, (HCOOH + K/Rh)–K/Rh (B). HCOOH exposure = 2.4 langmuirs.  $\theta_K = 0.1$ .  $T_a = 100$  K.

latter are very probably due to the formation of adsorbed CO.<sup>16</sup> They disappeared above 665 K.

When the Rh was covered by a larger amount of potassium ( $\theta_K = 0.36$ ), elimination of the 11.9-eV peak and the shift of the 6.2-eV peak to 5.2 eV were apparently complete at 213–230 K, when a new peak developed at 14–14.2 eV (Figure 8A). Attenuation of the peaks started at somewhat higher temperature, above 263 K, than in the previous case; the peaks were eliminated at around 422 K. New peaks at 8.4 and 11.9 eV characteristic of adsorbed CO were clearly identified first at 362 K in the difference spectra. They were seen in the spectra up to 667 K. The appearance of a not very well resolved new peak at 11.0 eV can be established at or above 422 which vanished only around 667 K.

The situation was different when the surface was covered only by a small amount of HCOOH (0.6 langmuir of HCOOH exposure). In harmony with the TD results (Figure 1B), the characteristic photoemission spectrum of adsorbed formate in this case developed already at 147 K (Figure 8B). A decrease in the

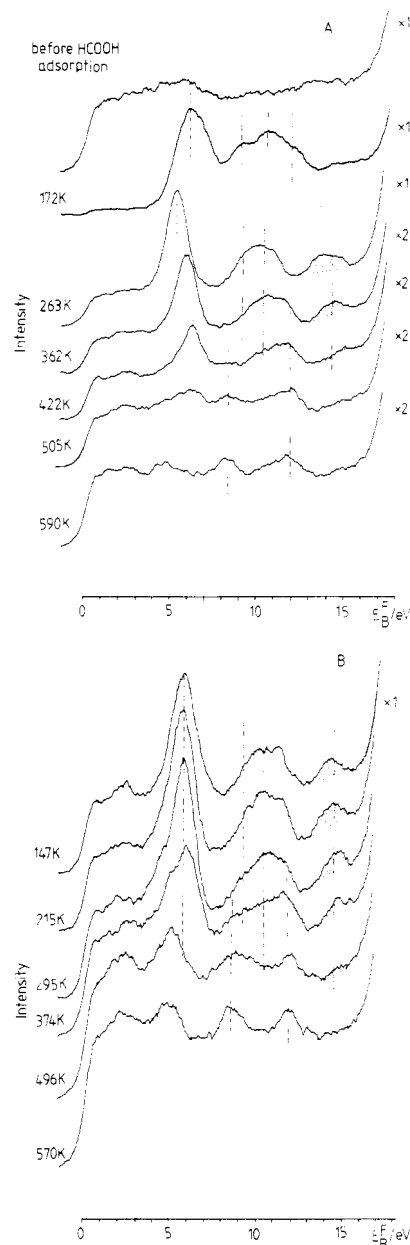


**Figure 8.** Effects of heating on the He II photoemission spectra of adsorbed HCOOH.  $\theta_K = 0.36$ .  $T_a = 100$  K. HCOOH exposure: 2.4 langmuirs (A) and 0.6 langmuirs (B).

intensity of the peaks occurred above 295 K and they were eliminated only at around 500 K; these changes were accompanied with the appearance of CO peaks.

**3. Work Function Measurements.** The work function changes observed following potassium deposition on a clean Rh(111) surface were reported in previous papers.<sup>3–5</sup> The work function of Rh decreased linearly with K exposure up to  $\theta_K = 0.17$ ,  $\Delta\phi = -3.5$  eV. Further K deposition led to a slight increase (0.5 eV) in  $\Delta\phi$ . The large linear decrease in the work function in the low K coverage range ( $\theta_K = 0.0$ – $0.17$ ) indicates the formation of a species with high dipole moment (formation of an “ionic” K). Above a potassium coverage of  $\theta = 0.17$  a strong dipole–dipole polarization starts to overcompensate the effect of the increasing K concentration (formation of a “metallic” potassium).

Whereas the adsorption of HCOOH on clean Rh resulted in a decrease ( $\Delta\phi = -0.75$  eV) in the work function, on a K-dosed surface it exerted an opposite influence. In the case of  $\theta_K = 0.36$ , the work function increase was preceded by a slight initial decrease (Figure 9A). Heating of the coadsorbed layer resulted in a complex picture (Figure 9B). First a decrease in the work function occurred in the temperature range 180–350 K, which corresponds to the desorption and decomposition of adsorbed HCOOH species.

(16) Peebles, D. E.; Peebles, H. C.; White, J. W. *Surf. Sci.* **1984**, *136*, 463.

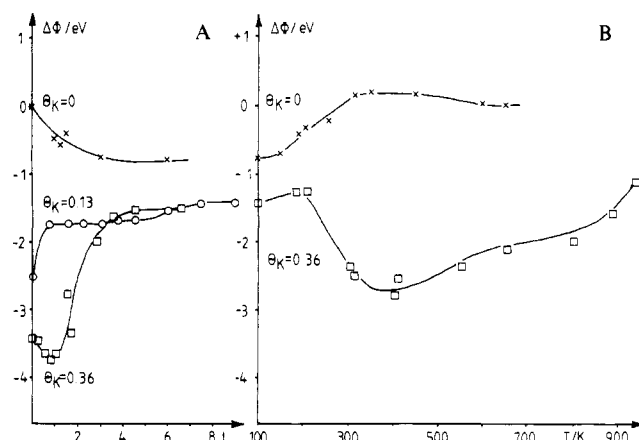


**Figure 9.** Changes in the work function following HCOOH adsorption on K-dosed Rh(111) surface at 100 K (A) and the effects of subsequent heating (B).

However, the  $\Delta\phi$  value was still higher than that observed before HCOOH adsorption, indicating that the products of surface reaction remained adsorbed on the surface. From 400 K the work function started to increase slowly. The original value for the clean Rh surface was attained only at 1150 K (Figure 9).

## Discussion

### 1. Main Features of HCOOH Adsorption on a Clean Rh(111).

Before a discussion of the effects of potassium, it is illuminating to survey the main features of HCOOH adsorption on clean Rh(111). HCOOH is adsorbed in an apparently random fashion on clean Rh(111) at 100 K, as no long-range order was found in LEED experiments. By means of TD measurements, three adsorption states were distinguished: a condensed layer ( $\alpha$ ,  $T_p = 170$  K), a chemisorbed state ( $\beta$ ,  $T_p = 202$  K), and an irreversibly adsorbed form, a formate species HCOO, which can be hydrogenated to HCOOH or decomposed to various products ( $\text{CO}_2$ ,  $\text{H}_2$ , CO, and  $\text{H}_2\text{O}$ ) at 200–250 K.<sup>1</sup>

The surface concentration of chemisorbed HCOOH at 100 K was  $6.9 \times 10^{14}$  molecules of HCOOH/cm<sup>2</sup>, from which about 90% decomposed to the above products. The ratio of the dehydrogenation and dehydration reactions depended on the coverage: at very low coverage, at  $\theta = 0.1$ , the  $\text{CO}_2/\text{CO}$  ratio was 0.5, while at saturation it was almost 4. Chemisorbed HCOOH was characterized in the He II photoemission spectrum by peaks at 6.2, 8.9, 10.5, 11.9, and 16.2 eV. The formation of the formate species was attributed to the appearance of a spectrum with four peaks, at 5.3, 8.6, 10.2, and 13.2 eV, which were assigned to  $1a_2$ ,  $6a_1$ ,  $4b_2$ ,  $3b_2$ ,  $5a_1$ , and  $4a_1$  orbitals of adsorbed formate.<sup>12–15</sup> This structure was present up to about 249 K. Above this temperature, new photoemission peaks developed at 8.1 and 11.2 eV, due to adsorbed CO produced in the surface decomposition.

**2. Main Features for Adsorption and Decomposition of HCOOH on K-Dosed Rh(111).** The TD measurements indicated that the amount of HCOOH desorbed in the  $\beta$  state slightly increased up to  $\theta_K = 0.15$ . The  $\beta$  peak became broad and asymmetric on the high-temperature side. The shape of the curve clearly demonstrated the existence of a more stable adsorbed state. A similar increase was observed in the surface concentration of the irreversibly adsorbed formate as indicated by the higher intensities of its photoemission peaks and by the increased amounts of  $\text{H}_2$  and  $\text{CO}_2$  formed at high temperature. The stability of formate species and the ratio of  $\text{CO}/\text{CO}_2$  were increased with the increase of the potassium coverage. The effect of potassium was also exhibited in the higher desorption temperatures of decomposition products.

Similarly as in our previous studies,<sup>3–5</sup> it is appropriate to discuss the effects of potassium at low ( $\theta_K \leq 0.1$ ) and at high coverages ( $\theta_K = 0.36$ ) separately, as the K/Rh systems behave differently at these coverages. As demonstrated by work function measurements on Rh(111),<sup>3–5</sup> and as established for other K + metal systems, potassium adatoms exhibit an ionic character at low

coverage, and a more metallic character at monolayer coverage.

**2.1.  $\theta_K < 0.1$ .** There is no doubt that at this low potassium coverage, HCOOH can still adsorb on the K-free Rh atoms; the adsorption state on this site is hardly influenced by the K additive. This is reflected in the unaltered section of desorption curves for HCOOH and for its decomposition products (Figures 1 and 2). As regards the enhanced dissociation on this surface we propose the following explanation.

For K-free Rh(111), the  $\beta$  state was attributed to the desorption of chemisorbed HCOOH



but the occurrence of the associative desorption of HCOOH and its contribution to HCOOH desorption was also considered:<sup>1</sup>



The work function changes for HCOOH on K-dosed Rh suggest a large negative charge on the chemisorbed molecule, which is probably due to the enhanced back-donation of electrons from the potassium-promoted Rh into an empty  $\pi$  orbital of HCOOH.

However, we may assume that this enhanced back-donation occurs directly between the formate and the K/Rh surface. The binding energy of the formate species is therefore increased and the probability of associative desorption (step 2) is decreased. This would result in a higher desorption temperature of the associative desorption and in a greater concentration of irreversibly adsorbed formate species, as was found in TD studies. The higher intensities of the four peaks at 5.2, 9.1, 10.0, and 14.2 eV, indicative of formation of the formate species,<sup>1,12–15</sup> also suggest that the amount of the formate species is larger than on the K-free surface.

Furthermore, these peaks exhibit a higher stability than in the case of the K-free surface; they can be detected up to about 330 K, whereas they completely vanish below 267 K from the spectrum of the K-free surface. This clearly indicates stabilization of the formate species even on the surface with  $\theta_K = 0.1$ .

The stabilization of H(a) by potassium ( $T_p$  is increased from 356 to 400 K<sub>4</sub>) can also hinder the associative desorption of HCOOH.

**2.2.  $\theta_K = 0.33$ .** As the nature of the interaction between HCOOH and K-dosed Rh (111) is dependent on the surface concentration of adsorbed HCOOH, it is instructive in this case too to discuss the results obtained at low and high surface concentrations separately.

**a. Low HCOOH Exposure (<1 langmuir).** In this case no desorption of HCOOH was detected. The surface concentration of adsorbed HCOOH corresponds to  $1.5 \times 10^{14}$  HCOOH molecules/cm<sup>2</sup>. As the surface concentration of adsorbed potassium at monolayer is  $5.75 \times 10^{14}$  potassium atoms/cm<sup>2</sup>,<sup>3</sup> the amount of potassium is  $\sim 4$  times larger than that of adsorbed HCOOH. Analysis of UPS spectra suggests that the adsorbed HCOOH is completely dissociated on this surface even at  $\sim 150$  K. The formate species formed exhibited marked thermal stability; its decomposition began above 300 K and was completed at  $\sim 500$  K (Figure 8B). The products of the surface decomposition were  $\text{H}_2$ , CO, and  $\text{CO}_2$  in nearly equal amounts, with some  $\text{H}_2\text{O}$  formation. However, these products desorbed at relatively high temperatures. From Figures 4 and 5, we obtain the following peak temperatures:  $T_p(\text{H}_2) = 483$  K,  $T_p(\text{CO}) = 706$  K,  $T_p(\text{CO}_2) = 637$  and 683 K, and  $T_p(\text{H}_2\text{O}) = 605$  K. It is important to mention that a portion of  $\text{H}_2$  also desorbed at 325–425 K.

For the interpretation of these features, we propose that a direct interaction between potassium and formic acid occurs, in which "potassium formate" like species is formed.

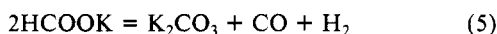
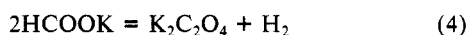


Bulk potassium formate is a relatively stable compound.<sup>17,18</sup> Its decomposition begins above 573 K and is characterized by two

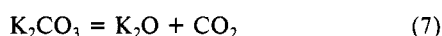
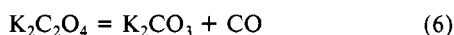
(17) Meisel, T.; Halmos, Z.; Seybold, K.; Pungor, E. *J. Thermal Anal.* **1975**, *7*, 73.

(18) Sabboh, J. R.; Bianco, P.; Habadjian, J. *Bull. Soc. Chim. Fr.* **1964**, *2304*.

simultaneously occurring reactions



which are complete by 723 K. Depending on the gas atmosphere, these reactions are followed by several secondary reactions at higher temperatures. In an inert atmosphere the most important ones are



Independently of the direction of the decomposition, the final product ratio ( $\text{H}_2:\text{CO}:\text{CO}_2$ ) is 1:1:1, which is in accord with the product distribution observed in the present case.

UPS studies provided no spectral evidence that the decomposition of potassium formate on the Rh surface occurs in a similar way, as we could not detect the photoemission peaks of either oxalate or carbonate. This could be due either to the low concentration of these surface compounds or to the strong overlapping of the  $\text{CO } 5\sigma/1\pi$  with the unresolved combination of  $3e'/1a_2''$  molecular orbitals of the  $\text{CO}_3$  species at 8.4 eV. Note that in this case we could not identify the photoemission peak at 5.5–6.0 eV (tentatively attributed to  $\text{K}-\text{OH}$ , see next section) which appeared at high  $\text{HCOOH}$  exposures at 290–590 K.

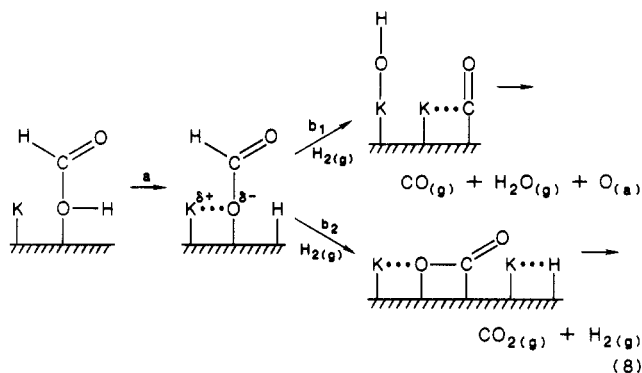
The fact that the decomposition of formate is completed at a lower temperature than that of the decomposition of bulk potassium formate is not in contradiction with this picture, as a similar lowering in decomposition temperature was observed for the decompositions of  $\text{K}_2\text{CO}_3$  on Fe foil<sup>19</sup> and  $\text{Rh}(111)$ ,<sup>3</sup> and of  $\text{Cs}_2\text{CO}_3$  on the  $\text{Ag}(111)$  surface.<sup>20</sup>

As regards the formation of gaseous species at high temperature, it must be borne in mind that potassium drastically increases the binding energy of all these gases to the Rh surface.<sup>3,4,21</sup> However, from a comparison of the peak temperatures with those found following the adsorption of these gases on a K-dosed  $\text{Rh}(111)$  surface,<sup>3,4,21</sup> it seems likely that the evolution of  $\text{H}_2$  ( $T_p = 483$  K) is a reaction-rate-limited process (steps 4 and/or 5) while that of  $\text{CO}$  is a desorption-rate-limited process. The hydrogen formed in the reaction between K and  $\text{HCOOH}$  (step 3) is somewhat stabilized by potassium and desorbed at 325–425 K. (The highest peak temperature we found for  $\text{H}_2$  desorption from K-dosed Rh at  $\theta_K = 0.36$  was 387–400 K.<sup>4</sup>)  $T_p$  values for  $\text{CO}_2$  formation agree well with those attributed to the decomposition of  $\text{K}_2\text{CO}_3$  on  $\text{Rh}(111)$ ,<sup>3</sup> which may support the above reaction scheme.

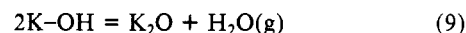
*b. High HCOOH Exposure (>1 langmuir).* With increase of the  $\text{HCOOH}$  exposure, the desorption of  $\text{HCOOH}$  also occurred (Figure 1). The intensities of the photoemission peaks due to formate species were somewhat higher, but they were eliminated at a lower temperature (at about 422 K) than in the previous case. This behavior suggests that as a result of the increased concentration of adsorbed formic acid or formate, which certainly leads to increase in the formate/K ratio on the surface, a destabilization of potassium formate occurred. This was exhibited in particular in a significant decrease in the amount of  $\text{H}_2$  desorbed in the high-temperature peak with  $T_p = 483$  K (Figure 4), which was attributed to the transformation of potassium formate to potassium oxalate or carbonate (eq 4 and 5). Similar features were observed in the case of the interaction of  $\text{CH}_3\text{OH}$  with a monolayer of potassium on  $\text{Rh}(111)$ : increase of the adsorbed  $\text{CH}_3\text{OH}$  clearly led to the destabilization of potassium methoxide.<sup>5</sup>

At higher  $\text{HCOOH}$  exposures, half of the  $\text{H}_2$  desorbed below 300 K ( $T_p = 280$  K), and the remainder at 320–450 K, and a significant amount of  $\text{H}_2\text{O}$  was also produced. This again suggests that at a high concentration of adsorbed  $\text{HCOOH}$  the nature of the interaction is basically changed. We may assume that in this

interaction the potassium stabilizes the formate in a monodentate mode.



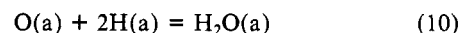
The  $\text{H}_2$  formed in the dissociation process (eq 8) desorbs in practically the same fashion as from the K-free surface. The formation of a strong  $\text{K}-\text{O}$  bond induces cleavage of the  $\text{C}-\text{O}$  bond, and as a result the production of  $\text{CO}$  comes into prominence. In the subsequent steps the  $\text{K}-\text{O}$  reacts with hydrogen, and the dehydration of two  $\text{K}-\text{OH}$  at higher temperatures leads to the enhanced formation of  $\text{H}_2\text{O}$ :



The shift of the photoemission peak from 5.2 to 6.2 eV above 290 K may be considered as a consequence of the formation of  $\text{OH}$  group (the oxygen lone pair of  $\text{OH}(\text{a})$  has a peak at  $\sim 5.5$ – $6.0$  eV<sup>22</sup>). A decrease in its intensity above 350 K and its elimination at 590 K corresponds to eq 9, i.e., to the evolution of  $\text{H}_2\text{O}$  from 350 to about 600 K (Figure 5A).

This change in the surface layer was not reflected in the desorption of  $\text{CO}$ , supporting the view that the evolution of  $\text{CO}$  from K-dosed  $\text{Rh}(111)$  is a desorption-rate-limited process. The fact that the amount of  $\text{CO}_2$  desorbed above 600 K increased indicates that  $\text{CO}_2$  formed in the surface decomposition of formate at lower temperature is stabilized by potassium, possibly in the form of a surface carbonate.

An alternative route for the enhanced formation of  $\text{CO}$  (and  $\text{H}_2\text{O}$ ) is that  $\text{CO}_2$  formed in the surface decomposition further dissociates to  $\text{CO}$  and  $\text{O}$ . Although  $\text{CO}_2$  adsorbs weakly and molecularly on a carefully cleaned  $\text{Rh}(111)$  surface,<sup>23</sup> potassium adatoms (besides stabilizing  $\text{CO}_2$  on  $\text{Rh}(111)$ ) induce the dissociation of  $\text{CO}_2$ .<sup>3</sup> The extent of dissociation at  $\theta_K = 0.3$  was also about 50% of adsorbed  $\text{CO}_2$ . Accordingly, the production of  $\text{H}_2\text{O}$  would be a result of the reaction between adsorbed  $\text{O}$  formed in the dissociation of  $\text{CO}_2$  and adsorbed hydrogen:



However, the probability of this reaction, at least on the clean surface, is very low.<sup>24</sup> Assuming that the situation is the same on K-dosed  $\text{Rh}(111)$ , we believe that this mode of formation of  $\text{CO}$  and  $\text{H}_2\text{O}$  presents only a minor pathway.

Thermal desorption data indicated that potassium is also greatly stabilized in the adsorbed layer (Figure 6), which suggests a strong interaction between potassium and adsorbed species. A similar mutual stabilization was observed following the adsorption of  $\text{CO}_2$ ,<sup>3</sup>  $\text{H}_2\text{O}$ ,<sup>4</sup>  $\text{CH}_3\text{OH}$ ,<sup>5</sup> and  $\text{NO}$ <sup>25</sup> on K-dosed  $\text{Rh}(111)$  surface. As the decomposition of formate is practically complete before the desorption of stabilized potassium occurs, the stabilization of potassium can be attributed to the interaction between the potassium and the decomposition products of surface reactions. It appears that the desorption of potassium with  $T_p = 590$  K is connected with the reaction 9, i.e., with the evolution of  $\text{H}_2\text{O}$ , whereas the high-temperature desorption,  $T_p = 690$  K, is associated with the release of  $\text{CO}$  or  $\text{CO}_2$ .

(19) Bonzel, H. B.; Broden, G.; Krebs, H. J. *Appl. Surf. Sci.* **1983**, *16*, 373.

(20) Grant, R. B.; Harblach, Ch.A.J.; Lambert, R. M.; Aun Tan, S. *Faraday Symp. Chem. Soc.* **1986**, *8*, 21.

(21) Crowell, J. E.; Somorjai, G. A. *Appl. Surf. Sci.* **1984**, *19*, 73.

(22) Benndorf, C.; Nöbl, C.; Madey, T. E. *Surf. Sci.* **1984**, *138*, 292.

(23) Solymosi, F.; Kiss, J. *Surf. Sci.* **1985**, *149*, 17.

(24) Thiel, P. A.; Yates, Jr. J. T.; Weinberg, W. H. *Surf. Sci.* **1979**, *90*, 121.

(25) Bugyi, L.; Solymosi, F. *Surf. Sci.* **1987**, *188*, 475.

## Conclusions

K adatoms significantly altered the adsorption and reactions of HCOOH on Rh surface. It led to the transformation of weakly held HCOOH to a more stable one ( $T_p = 254$  K), increased the surface concentration and stability of the formate species, and induced the cleavage of C-O bond. Analysis of the product distribution of the surface decomposition indicated that the effect

of the potassium differs at low ( $\theta_K \geq 0.1$ ) and at high ( $\theta_K = 0.36$ ) coverages. It is assumed that at high potassium coverage a direct interaction occurs between potassium and formic acid resulting in the formation of a stable "potassium formate" like species, which exists on the surface up to about 500 K. A destabilization of this surface compound was experienced at high formate/K ratio.

Registry No. Rh, 7440-16-6; K, 7440-09-7; HCO<sub>2</sub>H, 64-18-6.

## Hydrogen on MoS<sub>2</sub>. Theory of Its Heterolytic and Homolytic Chemisorption

Alfred B. Anderson,\* Zeki Y. Al-Saigh,<sup>†</sup>

Chemistry Department, Case Western Reserve University, Cleveland, Ohio 44106

and W. Keith Hall

Department of Chemistry, University of Pittsburgh, Pittsburgh, Pennsylvania 15260 (Received: May 22, 1987; In Final Form: September 9, 1987)

An atom superposition and electron delocalization molecular orbital study has been made of hydrogen adsorption on MoS<sub>2</sub>. We have calculated structures, binding energies, force constants, and frequencies. The most stable chemisorption form is heterolytic at edges of the crystal layers. Reductive homolytic adsorption on the sulfur anion basal planes is predicted to be less stable but is still predicted to occur up to a stoichiometry of H<sub>X</sub>MoS<sub>2</sub> where  $X \sim 1$ . For values of  $X$  greater than 1, the Mo conduction band is filled to such a level that further reduction by hydrogen becomes energetically unfavorable. H<sub>X</sub>MoS<sub>2</sub> should be a conducting bronze, according to our results. We propose that, under high H<sub>2</sub> pressures and at sufficiently high temperatures for H to diffuse over the anion surface (a 1.2-eV barrier is calculated), H can diffuse from edge sites out over the basal planes and the edges will be replenished by further heterolytic adsorption. We calculate a basal plane SH bending vibration at 431 cm<sup>-1</sup> and values for edge and corner SH and one MoH edge bond in the 500-600-cm<sup>-1</sup> range, thereby providing an interpretation for the time-, temperature-, and pressure-dependent inelastic neutron scattering vibrational spectra of Wright and co-workers.

## Introduction

Hydrogen gas adsorbs heterolytically on zinc oxide, ZnO, according to bond vibrational frequency measurements by Pliskin and Eischens<sup>1</sup> and Kokes and co-workers.<sup>2</sup> The surface hydrogen may be viewed as H<sup>-</sup> bonded to Zn<sup>2+</sup> to form ZnH<sup>+</sup> and H<sup>+</sup> bonded to O<sup>2-</sup> to form OH<sup>-</sup>. Anderson and Nichols<sup>3</sup> have shown in terms of the electronic structure of ZnO why heterolytic adsorption is favored over the homolytic alternatives. Zinc oxide has empty dangling surface orbitals several electronvolts higher in energy than the filled valence orbital energies. If two H atoms are bonded homolytically to two O<sup>2-</sup>, forming two OH<sup>-</sup>, two electrons are released and they will be promoted to the dangling surface orbitals or, if none are present, to the even higher lying bulk conduction band. This promotion energy makes homolytic adsorption on O<sup>2-</sup> sites unstable. Homolytic adsorption on Zn<sup>2+</sup> sites is also weak because each Zn<sup>2+</sup>-H bond has a formal bond order of only 1/2. Heterolytic adsorption leads to two single bonds without the energetic cost of electron promotion.

The above results and discussion would be expected to carry over to other metal oxides. As expected, Anderson and co-workers<sup>4</sup> predict that heterolytic adsorption of H<sub>2</sub> is strongly favored over homolytic adsorption on edge sites of MoO<sub>3</sub>, which has a gap of ~3 eV between the filled O 2p and empty Mo 4d valence bands. As these investigators show,<sup>5</sup> other single bonds are expected to dissociate similarly on MoO<sub>3</sub>, and in the case of methane, O<sup>-</sup> at the surface activates CH bonds readily. Kokes and co-workers<sup>6</sup> showed that C<sub>3</sub>H<sub>6</sub> chemisorbs in a similar fashion on ZnO, forming OH<sup>-</sup> and allylic intermediates bound to Zn<sup>2+</sup>.

It is, based on the above experimental results for ZnO and theoretical results for ZnO and MoO<sub>3</sub>, as well as vibrational studies

of hydrogen adsorption on MgO,<sup>7</sup> likely that single-bond cleavage will be heterolytic on any oxide or other metallic compound with a large band gap. An interesting question is what will be the mode or modes of hydrogen adsorption on materials with small filled-to-empty valence band gap? In the present study the binding of hydrogen to MoS<sub>2</sub> is examined in this regard.

A number of transition-metal sulfides are low band gap semiconductors. One of them, MoS<sub>2</sub>, is an important catalytic material for hydrogenation,<sup>8-10</sup> isomerizations,<sup>9-11</sup> and hydrodesulfurization<sup>12,13</sup> reactions. Despite the catalytic and technological importance of MoS<sub>2</sub>, the experimental evidence does not make clear how H<sub>2</sub> adsorbs. Burwell and co-workers<sup>14</sup> have pointed out that homolytic oxidative chemisorptions are known only for transition-metal ions in low valence states and have suggested,

- (1) Eischens, R. P.; Pliskin, W. A. *J. Catal.* **1962**, *1*, 80.
- (2) Kokes, R. J. *Acc. Chem. Res.* **1973**, *6*, 226.
- (3) Anderson, A. B.; Nichols, J. A. *J. Am. Chem. Soc.* **1986**, *108*, 4742.
- (4) Anderson, A. B.; Mehandru, S. P. *J. Am. Chem. Soc.*, in press.
- (5) Mehandru, S. P.; Anderson, A. B.; Brazdil, J. F.; Grasselli, R. K. *J. Phys. Chem.* **1987**, *91*, 2930.
- (6) Kokes, R. J.; Dent, A. L. *Adv. Catal.* **1972**, *22*, 1.
- (7) Ito, T.; Kuramoto, M.; Yoshioka, M.; Tokuda, T. *J. Phys. Chem.* **1983**, *87*, 4411.
- (8) Tanaka, K. I. *J. Chem. Soc., Faraday Trans. 1* **1979**, *75*, 1403. Tanaka, K. I.; Ohuhari, T. *Catal. Rev. Sci. Eng.* **1977**, *15*, 249.
- (9) Tanaka, K. I.; Okuhara, T. *J. Catal.* **1982**, *78*, 155.
- (10) Hall, W. K.; Millman, W. S. *Proceedings of the Seventh International Congress on Catalysis*; Tokyo, 1980; Part B, p 1304.
- (11) Hall, W. K. *Proceedings of the Fourth International Conference on the Chemistry and Uses of Molybdenum*, Barry, H. F.; Mitchell, T. C. H., Ed.; Climax Molybdenum Company: Ann Arbor, MI, 1982; pp 224-233.
- (12) Blake, M. R.; Eyre, M.; Moyes, R. B.; Wells, P. B. *Bull. Soc. Chim. Belg.* **1981**, *90*, 1293.
- (13) Blake, M. R.; Eyre, M.; Moyes, R. B.; Wells, P. B. *Proceedings of the Seventh International Congress on Catalysis*; Tokyo, 1980; Part A, p 591.
- (14) Burwell, R. L.; Stec, K. S. *J. Colloid Interface Sci.* **1977**, *58*, 54. Burwell, R. L.; Eley, S. R. *J. Colloid Interface Sci.* **1978**, *65*, 244.

\* Address correspondence to this author.

<sup>†</sup> Present address: Chemistry Department, University of Charleston, Charleston, WV 25304.